Parasitol Res (2015) 114:3327–3336
DOI 10.1007/s00436-015-4558-0

ORIGINAL PAPER

Morphological and molecular characterization of *Nosema pernyi*, a microsporidian parasite in *Antheraea pernyi*

Yong Wang[1] · Wei Liu[1] · Yiren Jiang[1] · Ling Huang[1] · Muhammad Irfan[2] · Shenglin Shi[1] · Ruisheng Yang[1] · Li Qin[1]

Received: 16 March 2015 / Accepted: 25 May 2015 / Published online: 6 June 2015

Abstract *Nosema pernyi* is a lethal pathogen that causes microsporidiosis in the Chinese oak silkworm, *Antheraea pernyi*. In this study, we presented its morphological and some molecular characteristics. The mature spores were measured to be 4.36×1.49 μm. The spore wall consisted of an electron-dense exospore (EX) and electron-lucent endospore (EN) layer. The polar filament (PF) was isofilar with 10–12 coils that were frequently arranged in a single row. Investigation results indicated that *N. pernyi* can infect the gut wall, silk glands, and other tissues. A full-length SMART cDNA library of *N. pernyi* was constructed, and then 824 expressed sequence tags (ESTs) were sequenced. Ninety unigenes, out of 197 assembled unigenes, showed significant homology to known genes of *Nosema ceranae*, *Nosema bombycis*, *Encephalitozoon cuniculi*, and other microsporidian species. Based on the nucleotide sequence of the α- and *β-tubulin* genes and amino acid sequence of *actin* gene, phylogenetic trees analysis showed that *N. pernyi* was closely related to *Nosema philosamiae* and *Nosema antheraeae*. It was correctly assigned to the *Nosema* group.

Yong Wang and Wei Liu contributed equally to this work.

✉ Li Qin
qinli1963@163.com

[1] College of Bioscience and Biotechnology, Liaoning Engineering and Technology Resource Center for Insect Resource, Shenyang Agricultural University, Shenyang 110866, People's Republic of China

[2] College of Plant Protection, Shenyang Agricultural University, Shenyang, Liaoning Province 110866, China

Keywords *Nosema pernyi* · Ultrastructure · EST · Phylogenetic analysis

Introduction

Microsporidia constitute a group of obligate intracellular eukaryotic parasites that infect invertebrates and vertebrates (Wittner and WeissWittner and Weiss 1999). The phylum microsporidia comprises nearly 1300 species belonging to 160 genera (Corradi et al. 2008). The microsporidia, with a distinct eukaryotic nucleus and nuclear envelope, also lack some typical eukaryotic characteristics such as mitochondria, and their ribosomes resemble those of prokaryotic organisms (Nageswara-Rao et al. 2004). The first microsporidian identified was *Nosema bombycis* Naegeli from the mulberry silkworm. Louis Pasteur suggested the use of spore-free mother moths to obtain healthy eggs, and this practice is still in use. Microsporidiosis remains a threat to the silk industry even in the modern times because of horizontal and vertical transmission of this disease (Bhat et al. 2009). The microsporidia have caused losses in livestock and have also been detected found in HIV-infected humans who developed microsporidiosis in an immunocompromised state (Didier 2005).

The Chinese oak silkworm, *Antheraea pernyi* (Lepidoptera: Saturniidae), is a well-known wild silk moth used for silk production, and is an important food source for people in many countries. This insect is commercially cultivated in China, Korea, and India. The annual output of oak silkworm cocoons approximately 8×10^4 t from China accounts for 90 % of wild silk production all over the world (Liu et al. 2010). The rearing of oak silkworm is the main source of income in most sericultural areas. However, the deleterious

effects of microsporidiosis have significantly affected this industry in these areas.

As a new parasite species identified in the Liaoning province of China, *Nosema pernyi* Wen et Ding can cause microsporidiosis in *A. pernyi*. This pathogen infects the midgut epithelium, silk glands, muscle tissues, fat body, blood cells, and reproductive organs of *A. pernyi*. The Malpighian tubules and neurons are occasionally infected, and a small number of microsporidian spores were found within these structures (Su et al. 1992). There are reports showing differences in spore production and infection when comparing infection with *N. pernyi* to that with *Nosema antheraeae*, the other described Chinese oak silkworm microsporidian parasite (Su et al. 1992). To provide a preliminary analysis of *N. pernyi*, light and electron microscopic examinations were carried out. A full-length cDNA library using purified *N. pernyi* spores was constructed, and 864 expressed sequence tags (ESTs) were sequenced. In order to analyze the phylogenetic relationship between *N. pernyi* and other microsporidian species, *α-tubulin*, *β-tubulin*, and *actin* genes were used to construct a phylogenetic tree in this study. Our results contribute to a better understanding of *N. pernyi*, a microsporidian isolated from *A. pernyi* in Northeast China.

Materials and methods

Materials

N. pernyi were housed at the Research Institute for Tussah, Shenyang Agricultural University (Shenyang, China). *N. pernyi* were purified from the infected larvae of the Chinese oak silkworm variety ShenHuang No.2, using Percoll (Amersham Pharmacia Biotech, Piscataway, NJ, USA) density gradient centrifugation ultracentrifuge (Hitachi, Tokyo, Japan), as described previously (Jiang et al. 2011). *A. pernyi* larvae infected with *N. pernyi* were chopped in phosphate-buffered saline (PBS), and 2 ml of the suspension was layered onto a gradient containing 25, 50, and 75 % Percoll in PBS and 100 % Percoll (2 ml of each). The gradients were spun at 15,000×*g* for 30 min. Spores at the lowest layer were washed by repeated centrifugation in PBS.

Preparation for electron microscopy

The purified spores were examined using a light microscope (Olympus, Tokyo, Japan) fitted with an ocular micrometer and were photographed with ScopePhoto software (Version 3.0, Liyang Co., Ltd, Chengdu, China). Scanning electron microscopy (SEM) was performed as previously described (Schottelius et al. 2000), using a scanning electron microscope (S-450, Hitachi, Tokyo, Japan). For transmission electron microscopy (TEM), *N. pernyi* were fixed for 12–24 h with 2.5 % glutaraldehyde in 0.1 M sodium cacodylate buffer, pH 7.2 at 4 °C and then fixed for 1 h with 1 % osmium tetroxide. After dehydration in an ethanol series and propylene oxide, the fragments were embedded in an Epon resin and sectioned using a Reichert-Jung ultramicrotome. Sections were stained with uranyl acetate and lead citrate and observed under a H-7650 TEM (Hitachi, Tokyo, Japan) at an accelerating voltage of 80 kV (Liu et al. 2012; Wu et al. 2008).

cDNA library construction and EST analysis of *N. pernyi*

Total RNA was extracted by the CTAB method. Using the SMART cDNA Library Construction Kit (Clontech, Tokyo, Japan), a cDNA library of *N. pernyi* was constructed. Eight hundred and sixty-four clones were sent to BGI (Tianjin, China) for sequencing using a 3730xl DNA analyzer (Applied Biosystems, Foster city, CA, USA). Vectors and adapter sequences were removed using the crossmatch program (http://www.phrap.org/). High-quality ESTs (>100 bp) were assembled into contigs (contiguous sequences) using the Phrap program. Singlets (ESTs that could not be assembled together) and contigs were compared with nucleotide and protein sequences in databases using BLASTn and BLASTx (http://www.ncbi.nlm.nih.gov/), the Swiss-Prot database (http://www.expasy.ch/), and the KEGG database (http://www.genome.jp/).

Phylogenetic analysis

The *α-tubulin*, *β-tubulin*, and *actin* genes of *N. pernyi* were cloned using RT-PCR technology based on EST sequences from the constructed cDNA library. The *α*- and *β-tubulin* genes were combined for phylogenetic analysis. Other nineteen available microsporidian sequences were retrieved from the NCBI GenBank. *Dictyostelium discoideum* was used for comparison as an out group. Amino acid sequences of actin gene were used to construct a phylogenetic tree. Twelve species of microsporidia in GenBank were used in phylogenetic analysis. All sequences were aligned following the ClustalX 1.83 program. The tubulin phylogenetic tree based on the maximum likelihood (ML) was constructed using the MEGA 5.0 program (Tamura et al. 2011). Phylogenetic analysis of actin protein sequences was performed by neighbor-joining (NJ) method. One thousand bootstrap replicates were assessed to test the robustness of the tree.

Results and discussion

Pathogenic characteristics

In the late stages of infection, the infected larvae showed obvious symptoms of disease. The symptoms of microsporidiosis in *A. pernyi* include black spots that appear

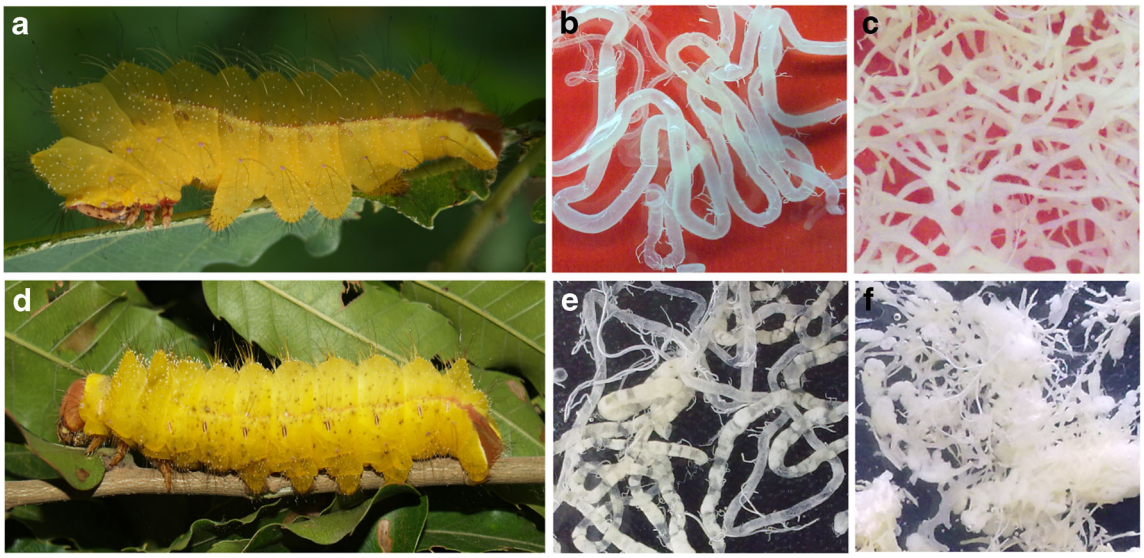

Fig. 1 The comparison between healthy and microsporidia-infected larva and tissues of *A. pernyi.* **a** Uninfected larva. **b** Uninfected silkgland. **c** Uninfected fatbody. **d** Infected larva. **e** Infected silkgland. **f** Infected fatbody

all over the surface of the insect body in the late infection period (Fig. 1d) compared with healthy larva (Fig. 1a). These black pepper-like spots were the hypodermal cells of infected larvae, which become enlarged and vacuolated, and blackened due to the formation of melanin (Velide and Bhagavanulu 2012). Investigation results indicated that *N. pernyi* can infect the gut wall, silk glands, blood cells, Malpighian tubes, muscles, ovary, nerves, and epidermis (Su et al. 1992). Some insects died prematurely, often in their second- or third-instar. The surviving larvae exhibited symptoms such as diarrhea and showed significant changes in the cocoon and shell weight. These changes were also observed during *Bombyx mori*, *Philosamia cynthia ricini*, and *Antheraea mylitta* breeding (Bhat and Nataraju 2005; Velide and Rao 2011). The midgut was first infected by the polar filament (PF) extruded from the spores in an alkaline environment. The infective sporoplasm penetrated the midgut cells (Tokarev et al. 2010). Anterior, middle, and posterior silk glands with pustule-like plaques were observed (Fig. 1e) compared with a healthy silk moth (Fig. 1b). Cocooning was prevented because fibroin secretion was destroyed by the infection. The fat body was tumor-like, deformed, and with histolysis (Fig. 1f) compared with a healthy one (Fig. 1c). Plenty of spores were washed into the blood tissue, rendering it "muddy." At this point, the spores could be detected by light microscopy.

Light and electron microscopy observations

Light microscopy was used for morphological observation (Fig. 2a). The spores are the last development stage of the microsporidia. The mean length and width measurements for *N. pernyi* were 4.36±0.42 and 1.49±0.19 μm, respectively. The spores measured on the light micrographs of fresh spores were slightly larger.

Using a scanning electron microscope, the spots were enlarged to 14,500× (Fig. 2b, c). Transmission electron microscopy of longitudinal sections and cross-sections of spores revealed that the spore wall consisted of an electron-dense exospore (EX) and electron-lucent endospore (EN) layer. The sporoplasm was enclosed by a plasma membrane. The diplokaryotic nuclei occupied the center of the spore and were surrounded by 10–12 turns of the polar tube. Mature spores contained a lamellar polaroplast (PP) that was not typically visible, and a relatively small and inconspicuous polar vacuole (PV) was observed in the posterior region (Fig. 2d). Methanol-fixed spores were measured in length and width, averaging 3.096±0.206 and 1.33±0.13 μm (TEM), respectively, which was smaller than the fresh spores. Both light and electron microscopy was used to study infection with this pathogen in *A. pernyi*. Measurements taken during electron microscopy using fixed or stained preparations may be slightly different from those of fresh spores.

This pathogen belongs to the genus *Nosema* of microsporidia, which have several characteristics same with *Nosema*: a thin endospore with a moderately thick exospore and a distinctive, small posterior vacuole; all stages develop in the host cell cytoplasm, and diplokaryotic spores have an isofilar polar filament (Sprague et al. 1992). Meronts of *N. pernyi* were spherical and primarily diplokaryotic or tera-diplokatyotic (Li et al. 2005). Sporonts were round to oval with fused diplokaryotic nuclei, which is typical for microsporidia in the genus *Nosema*.

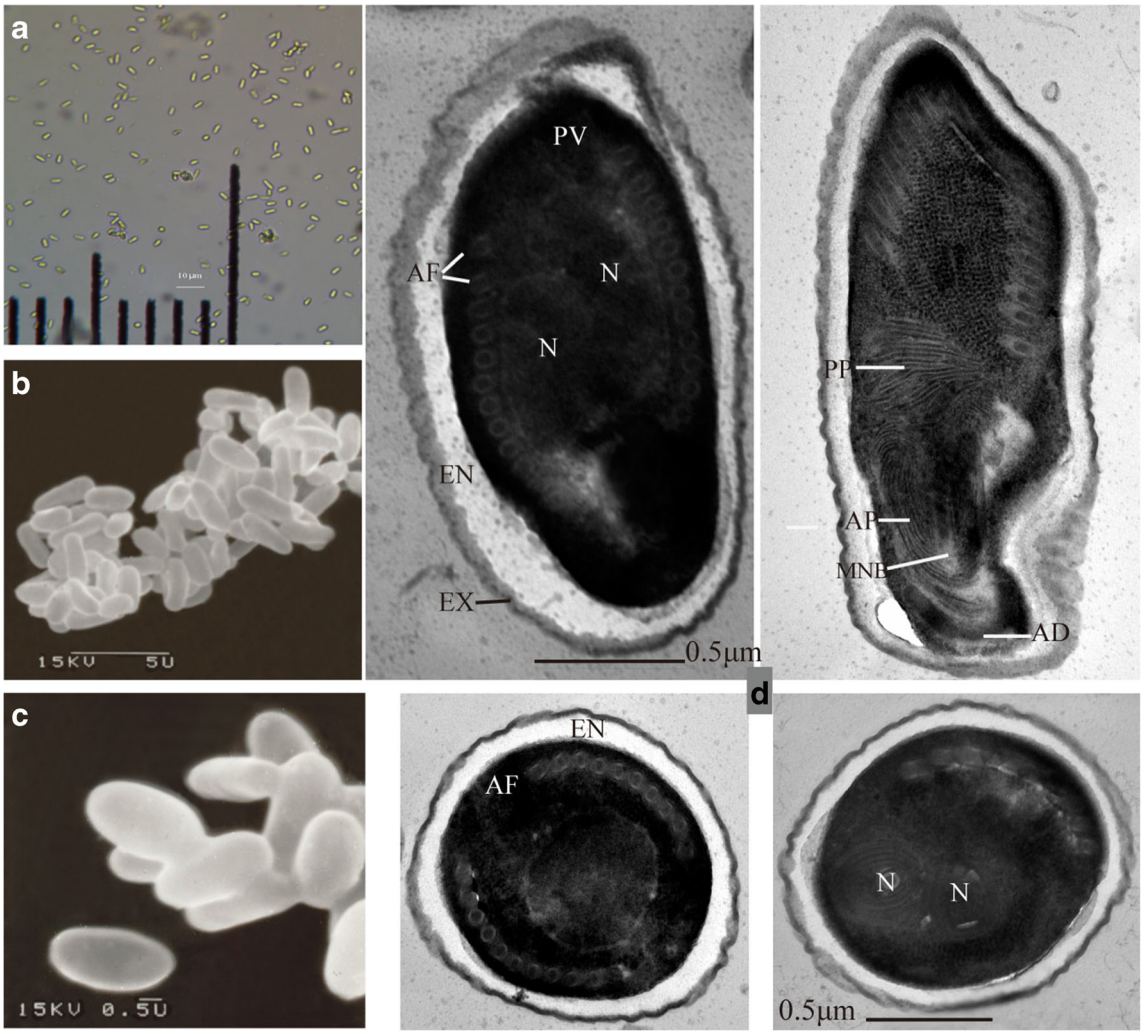

Fig. 2 Micrographs of *N. pernyi* spores. **a** Light micrograph of *N. pernyi* spores after Percoll purification (*Scale bar*=10 μm). **b** Scanning electron microscope micrograph of *N. pernyi* (*Scale bar*=5 μm). **c** Scanning electron microscope micrograph of *N. pernyi* (*Scale bar*=0.5 μm). **d** Transmission electron microscopy micrograph of *N. pernyi* (*Scale bar*= 0.5 μm). Longitudinal section and cross-section of *N. pernyi* spores, showing the exospore (*EX*), endospore (*EN*), nucleus (*N*), polar filament (*PF*), anchoring disc (*AD*), anterior region (*AP*), polaroplast (*PP*), manubroid (*MNB*), and posterior vacuole (*PV*)

cDNA library construction and EST analysis

A full-length cDNA Library was constructed. The primary titer of the library was 4.2×10^6 pfu/ml, and the insertion efficiency was assessed to be 98.39 %. The library capacity was 1.0×10^7 pfu. The sizes of the inserts, based on 32 randomly selected recombinant plasmids in the primary library, ranged from 750 to 3000 bp with an average length of 1000 bp, as measured by PCR amplification.

Random sequencing of 864 clones yielded 824 ESTs. After trimming the vectors, adapters, and low-quality sequences (<100 bp), 626 high-quality ESTs (>100 bp) were assembled into 197 unigenes containing 129 singlets and 68 contigs. About 346 ESTs lied in between 701 and 800 bp, accounting for 55.27 % of total ESTs. ESTs' length and frequency redundancy were analyzed. Some ESTs have repeated for many times, which indicated the genes expression in the spores of *N. pernyi*. Sixty-eight contigs consisting of 2-94 ESTs constituted 34.52 % of total unigene (68 of 197) and 79.39 % of total ESTs (497 of 626). There are 2 contigs, the replication of them are more than 50 times, in which the maximum is up to 94 times in the ESTs' sequencing. One hundred and twenty-nine singlets were unique sequences consisting of 65.48 % of total unigene (129 of 197) and 20.6 % of total ESTs (129 of 626). The occurrence rate of these singlets is only once in the present study.

These 197 unigenes were classified into three groups, "known genes," "putative genes," and "unknown genes." Ninety Unigenes showed homology to known genes in the Nr, Nt, Swiss-Prot, and KEGG database, with an *E* value cut-off 1.00E–5. Sixty-six putative genes shared a high degree of similarity with the proteins described as "putative," "like,"

or "similar to" in public databases. Forty-one unknown genes showed no sequence homology to sequences in the public databases, and they were termed "hypothetical proteins." One hundred and twenty-one genes were sequenced from the 5 to 3 ends using Sanger sequencing. These sequences containing complete open reading flame (ORF) have been submitted to the GenBank (Accession Nos. KJ210677 to KJ210797).

BLAST analysis of 197 ESTs indicated that 90 ESTs showed significant homology to known genes in the NCBI database (Table 1). These unigenes, which encoded spore wall proteins, translation initiation factor, elongation factor and termination factor, DNA replication factor, enzymes, and structural proteins, shared homology with sequences from *Nosema ceranae*, *N. bombycis*, *Encephalitozoon cuniculi*, and other microsporidian species.

The genome sizes of various microsporidian species vary significantly, ranging from 2.3 M (*Encephalitozoon intestinalis*) to 19.6 M (*Glugea atherinae*) (Keeling and Slamovits 2004). With no information about the genomic sequence of *N. pernyi* and great variation in the genome of different microsporidia genome, cDNA library construction in combination with EST analysis is an efficient approach for the collection of genomic information and identification of useful genes (Phukon et al. 2012). An EST analysis based on a cDNA library is an effective strategy for examining the expression patterns of genes (Zhou et al. 2011).

High-throughput sequencing has been extensively applied in genome sequencing and transcriptome sequencing because of its increased efficiency and low cost (Mardis 2008). However, this technology is not suitable for every species. Due to a strongly AT-biased genome (74 % A+T) and diversity of repetitive elements in microsporidia, assembly is a complicated process (Cornman et al. 2009). The assembled frame genome of *N. bombycis* has been shown to be dispersive and incomplete using high-throughput sequencing (Xu et al. 2010). Further, fine mapping can be done with the aid of the BCA library (Yang et al. 2009). Library construction is also used as an efficient measure for gene screening and gene expression examination in a given tissue or at a specific developmental stage (Zhou et al. 2011). In this study, we constructed an *N. pernyi* cDNA library and analyzed the ESTs, which proved to be an efficient method of studying the dominant microsporidian species infecting *A. pernyi* in Liaoning Province of China.

Phylogenetic analysis by using the *α-tubulin*, *β-tubulin*, and *actin* genes of *N. pernyi*

Using RT-PCR technology, the *α-tubulin*, *β*-tubulin, and *actin* genes of *N. pernyi* were cloned (the GenBank accession numbers were KF154086, KF023271, and KP677559). The cDNA sequence of *α-tubulin* gene with an ORF of 1323 bp and encodes 440 amino acids with predicted molecular mass of 49.21 kDa and theoretical isoelectric point of 5.48. *Beta-tubulin* gene with an ORF of 1299 bp and encodes 439 amino acids with predicted molecular mass of 49.36 kDa and theoretical isoelectric point of 4.91. The *Actin* gene of *N. pernyi* has an ORF of 1128 bp encoding 375 amino acids, and the predicted molecular mass of this protein is 42.23 kDa and isoelectric point is 5.83.

To examine the phylogenetic relationships between *N. pernyi* and other microsporidian species, the *α*- and *β-tubulin* genes of *N. pernyi* were combined, and sequences of 19 other microsporidian species were collected from the GenBank. The inferred ML-tree (Fig. 3) generated the same topology as the neighbor-joining (NJ) tree (not shown). Some relationships were recovered as expected; that is, Lepidoptera-infecting species were found to be the most closely related and tended to form a clade. From all the 19 microsporidian species analyzed, *N. pernyi* together with other species of the *Nosema* genus belongs to one of two groups. It has a closer relationship with *N. antheraeae* and *Nosema philosamiae*. Tubulin trees suggested that *Antonospora locustae* was transferred from the *Nosema* genus, and is evolutionarily closer to *Edhazardia aedi* and other *Encephalitozoon* species. Furthermore, this result also is supported by phylogenetic analysis based on amino acid sequence of the *actin* gene (Fig. 4). *N. pernyi* was closely related to *N. bombycis* and is correctly assigned to the *Nosema* group.

Microsporidia are small single-celled, obligate intracellular parasites that were considered to be early-branching eukaryotic protozoa based on the presence of prokaryote-like ribosomes, and the apparent absence of true Golgi, peroxisomes, and mitochondria, but now are reclassified with the fungi (Franzen 2008). The microsporidian genome has been found to be highly reduced, and mature organisms contained mitochondrion-derived organelles, or mitosomes. Golgi-like membranes and peroxisome-like organelles have also been identified (Williams et al. 2002).

Early classification of microsporidia was based on morphological characteristics, pathological symptoms, and the life cycle. However, using morphological characteristics often was difficult while dealing with closely related species (Wittner and Weiss 1999). Genes encoding conserved proteins have been used in the taxonomic determination. Based on LSU rRNA, ITS, SSU rRNA, IGS, and RPB1, the molecular marker for phylogenetic analysis among eukaryotes, many microsporidian species have been identified (Cheney et al. 2001; Zhu et al. 2011; Liu et al. 2015). Vast majority of molecular analyses of fungal phylogeny have focused on rRNA, similar conclusions will get from the same regions of the tree (Tanabe et al. 2000). Phylogenetic studies required evidence of concerted evolution in the multi-copy rRNA genes, converted to single copy genes with appropriate base substitution rates. Ribosomal genes share the same paralog with another,

Table 1 Ninety ESTs shared significant similarities with known genes of other species

Unigenes code	Sequence description/putative protein	Homology organism/matched species	GenBank match/ homology ID	Identity (%)	*E* value
contig10	Glutamate-cysteine ligase	*Nosema bombycis* CQ1	EOB14747.1	86	3.00E-45
contig12	White-brown complex protein 7-like protein	*Nosema bombycis* CQ1	EOB12393.1	87	3.00E-43
contig16	Zonadhesin	*Nosema bombycis* CQ1	EOB14289.1	61	5.00E-78
contig19	Structural maintenance of chromosomes protein 5	*Nosema bombycis* CQ1	EOB15517.1	98	3.00E-73
contig20	Exosome complex exonuclease RRP40	*Nosema bombycis* CQ1	EOB11348.1	91	3.00E-55
contig21	Spore wall protein 12	*Nosema antheraeae*	AFY13597.1	96	4.00E-63
contig22	Actin	*Nosema bombycis* CQ1	EOB14404.1	97	2.00E-68
contig25	Vacuolar transporter chaperone 4	*Nosema bombycis* CQ1	EOB14139.1	71	3.00E-43
contig29	DNA-directed RNA polymerase II subunit RPB1	*Nosema bombycis* CQ1	EOB12667.1	85	3.00E-71
contig30	Elongator complex protein 3	*Nosema bombycis* CQ1	EOB14850.1	87	2.00E-90
contig31	Transcription initiation factor TFIII B subunit (70kD)	*Encephalitozoon cuniculi*	NP_597392.1	45	2.00E-11
contig32	Ribonucleoside-diphosphate reductase small chain	*Nosema bombycis* CQ1	EOB15312.1	95	2.00E-62
contig33	Translation elongation factor EF-1 alpha	*Encephalitozoon hellem*	XP_003887492.1	41	4.00E-38
contig34	Spore wall protein	*Nosema bombycis*	ABV48892.1	72	3.00E-46
contig36	Translation initiation factor eIF-2B subunit epsilon	*Nosema bombycis* CQ1	EOB11891.1	94	3.00E-67
contig38	Solute carrier family 2, facilitated glucose transporter member 1	*Nosema bombycis* CQ1	EOB15272.1	75	3.00E-43
contig39	Elongation factor 1 alpha	*Nosema apis* BRL 01	EQB61867.1	72	2.00E-40
contig43	Spore wall protein 8	*Nosema antheraeae*	AEM23899.1	89	1.00E-60
contig44	Zinc finger C2H2 protein	*Nosema bombycis* CQ1	EOB11399.1	73	5.00E-39
contig46	Myosin heavy chain	*Nosema bombycis* CQ1	XP_003072746.1	72	5.00E-20
contig47	Beta-adaptin	*Nosema bombycis* CQ1	EOB11312.1	65	1.00E-23
contig50	ATP-dependent Clp protease heat shock protein 101	*Nosema bombycis* CQ1	EOB15389.1	97	2.00E-66
contig52	Structural maintenance of chromosomes protein 5	*Nosema bombycis* CQ1	EOB15517.1	56	3.00E-34
contig53	1-acyl-sn-glycerol-3-phosphate acyltransferase zeta	*Nosema bombycis* CQ1	EOB15471.1	89	3.00E-48
contig55	Phospholipid hydroperoxide glutathione peroxidase	*Nosema bombycis* CQ1	EOB14819.1	69	2.00E-50
contig56	Protein kinase domain protein-containing protein	*Nosema bombycis* CQ1	EQB60132.1	76	4.00E-38
contig57	Ribosomal protein l24e	*Nosema apis* BRL 01	EQB60132.1	76	2.00E-52
contig58	WD repeat-containing protein, partial	*Nosema bombycis* CQ1	EOB12184.1	97	1.00E-66
contig60	Spore wall protein 12	*Nosema antheraeae*	AFY13597.1	96	2.00E-56
contig65	Spore wall protein 30 gb|ABV48889.1|	*Nosema bombycis*	B3STN5.1	75	2.00E-46
contig66	Protein kinase domain protein-containing protein	*Nosema bombycis* CQ1	EOB14819.1	69	2.00E-50
contig67	Large subunit ribosomal RNA	*Nosema bombycis*	EJY66653.1	100	0.00E+00
contig68	UTP-glucose-1-phosphate uridylyltransferase	*Nosema bombycis* CQ1	EOB14930.1	90	3.00E-68
01_B04	GATA zinc finger domain-containing protein	*Nosema bombycis* CQ1	EOB14198.1	83	2.00E-46
01_C07	Acetyl-coenzyme A synthetase	*Nosema bombycis* CQ1	EOB12833.1	93	2.00E-67
01_D08	Helicase SKI2W	*Nosema bombycis* CQ1	EOB13350.1	95	1.00E-57
01_E01	Vacuolar protein sorting-associated protein 13a	*Nosema bombycis* CQ1	EOB13634.1	86	2.00E-58
01_F02	Thioredoxin reductase	*Nosema bombycis* CQ1	EOB13265.1	96	2.00E-49
01_F04	MADS domain-containing protein, partial	*Nosema bombycis* CQ1	EOB13319.1	61	3.00E-19
02_B03	Deoxyhypusine hydroxylase	*Nosema bombycis* CQ1	EOB15169.1	91	2.00E-56
02_B04	Myosin heavy chain	*Encephalitozoon hellem*	XP_003887123.1	69	3.00E-36
02_B12	Beta tubulin	*Encephalitozoon intestinalis*	XP_003072575.1	88	1.00E-44
02_D06	Adenylate kinase	*Nosema bombycis* CQ1	EOB14122.1	87	2.00E-91
02_E10	PRE-mRNA splicing helicase	*Nosema bombycis* CQ1	EOB13546.1	82	4.00E-18
02_G02	ATPase	*Nosema bombycis* CQ1	EOB13741.1	97	2.00E-74
02_H02	26S proteasome regulatory subunit RPN2	*Nosema bombycis* CQ1	EOB15425.1	89	4.00E-54
02_H03	60S ribosomal protein L3-like	*Bombus terrestris*	XP_003400694.1	51	2.00E-27

Table 1 (continued)

Unigenes code	Sequence description/putative protein	Homology organism/matched species	GenBank match/ homology ID	Identity (%)	*E* value
02_H09	Tristetraproline	*Nosema bombycis* CQ1	EOB12059.1	93	3.00E-66
03_B02	Chromosome segregation protein	*Encephalitozoon intestinalis*	XP_003072331.1	39	1.00E-17
03_C02	Ribose-5-phosphate isomerase A	*Nosema bombycis* CQ1	EOB13865.1	89	1.00E-67
03_C07	Midasin	*Nosema bombycis* CQ1	EOB15466.1	95	2.00E-53
03_D01	Queuine tRNA-ribosyltransferase	*Nosema bombycis* CQ1	EOB11176.1	97	3.00E-69
03_D08	Replication factor C subunit 2	*Nosema bombycis* CQ1	EOB14077.1	94	2.00E-48
03_E01	Methionyl-tRNA synthetase	*Nosema bombycis* CQ1	EOB15349.1	77	1.00E-33
03_F06	Small ubiquitin-related modifier 3	*Nosema bombycis* CQ1	EOB14736.1	96	4.00E-57
03_G10	Polar tube protein 3	*Nosema bombycis* CQ1	EOB15062.1	85	2.00E-46
03_H01	Chromodomain-helicase-DNA-binding protein 9	*Nosema bombycis* CQ1	EOB14309.1	91	5.00E-51
04_A04	T-complex protein 1 subunit epsilon	*Nosema bombycis* CQ1	EOB13574.1	91	2.00E-62
04_A10	Elongator complex protein 3	*Nosema bombycis* CQ1	EOB14850.1	98	4.00E-45
04_C04	Gamma tubulin	*Nosema pernyi*	AHG26159.1	100	0.00E+00
04_E06	Protein kinase C-like protein	*Nosema bombycis* CQ1	EOB14168.1	79	2.00E-45
04_E08	Spore wall protein 13	*Nosema bombycis* CQ1	EOB15261.1	64	3.00E-35
04_H09	Protein phosphatase 1 regulatory subunit 7	*Nosema bombycis* CQ1	EOB13753.1	72	2.00E-91
05_D07	Replication factor C subunit 4	*Nosema bombycis* CQ1	EOB11316.1	94	1.00E-75
05_H09	WD repeat and SOF domain-containing protein 1	*Nosema bombycis* CQ1	EOB14200.1	95	2.00E-66
05_H11	RNA polymerase II subunit A C-terminal domain phosphatase ssu72	*Nosema bombycis* CQ1	EOB12435.1	90	4.00E-65
06_A03	Anti-telomeric silencing protein	*Nosema bombycis* CQ1	EOB12474.1	76	2.00E-39
06_A04	P-ATPase-V	*Encephalitozoon romaleae* SJ-2008	AFN82499.1	55	3.00E-22
06_D05	WD-repeat protein	*Nosema bombycis*	ABW91183.1	95	4.00E-51
07_C07	Mitogen-activated protein kinase kinase kinase ANP1	*Nosema bombycis* CQ1	EOB13873.1	79	1.00E-34
07_E03	Ribosome maturation protein SBDS	*Nosema bombycis* CQ1	EOB14920.1	90	2.00E-47
07_E11	Chromodomain-helicase-DNA-binding protein 9	*Nosema bombycis* CQ1	EOB11679.1	93	2.00E-55
07_F06	Mitochondrial protein import protein MAS5	*Nosema bombycis* CQ1	EOB14160.1	82	1.00E-35
07_H04	Signal recognition particle receptor subunit alpha	*Nosema bombycis* CQ1	EOB15491.1	86	2.00E-60
08_A01	Spore wall protein	*Nosema bombycis*	ABV48897.1	83	3.00E-42
08_A07	Glucose transporter type 3	*Nosema bombycis* CQ1	EOB11546.1	28	2.00E-40
08_A08	Phospholipid-transporting ATPase IIA	*Nosema bombycis* CQ1	EOB14045.1	97	1.00E-71
08_B02	Elongation factor 2	*Nosema bombycis* CQ1	EOB15403.1	97	3.00E-61
08_B07	Zinc finger protein	*Nosema bombycis* CQ1	EOB15030.1	93	2.00E-48
08_C06	Nucleotide-sugar transporter	*Nosema apis* BRL 01	EQB61629.1	51	1.00E-25
08_D01	Phosphatidate cytidylyltransferase	*Nosema bombycis* CQ1	EOB13934.1	96	3.00E-61
08_E03	Vacuolar ATP synthase catalytic subunit A	*Nosema bombycis* CQ1	EOB12563.1	98	2.00E-54
08_E04	Peptidyl-prolyl cis-trans isomerase	*Nosema bombycis* CQ1	EOB14559.1	78	1.00E-86
08_E05	Structural maintenance of chromosomes protein 4	*Nosema bombycis* CQ1	AGE95781.1	72	2.00E-50
08_E10	Replication factor C small subunit	*Encephalitozoon hellem*	XP_003886760.1	52	2.00E-68
09_C03	60S ribosomal protein L5	*Nosema bombycis*	ADZ95732.1	59	2.00E-51
09_C07	Alpha-tubulin	*Nosema philosamiae*	ADF47157.1	99	1.00E-75
09_G09	40S ribosomal protein S5	*Nosema bombycis*	ADZ95657.1	98	2.00E-62
09_G10	Pol polyprotein	*Nosema bombycis*	ABE26655.1	47	2.00E-41
09_H02	Eukaryotic translation initiation factor 2C 2	*Nosema bombycis* CQ1	EOB14115.1	96	1.00E-64

and divergence between them may be just 2 % (Lahr et al. 2011). Due to the high rRNA copy number in microsporidia, rRNA may not be the best choice for the phylogenetic analysis (O'Mahony et al. 2007). Protein coding genes were chosen for

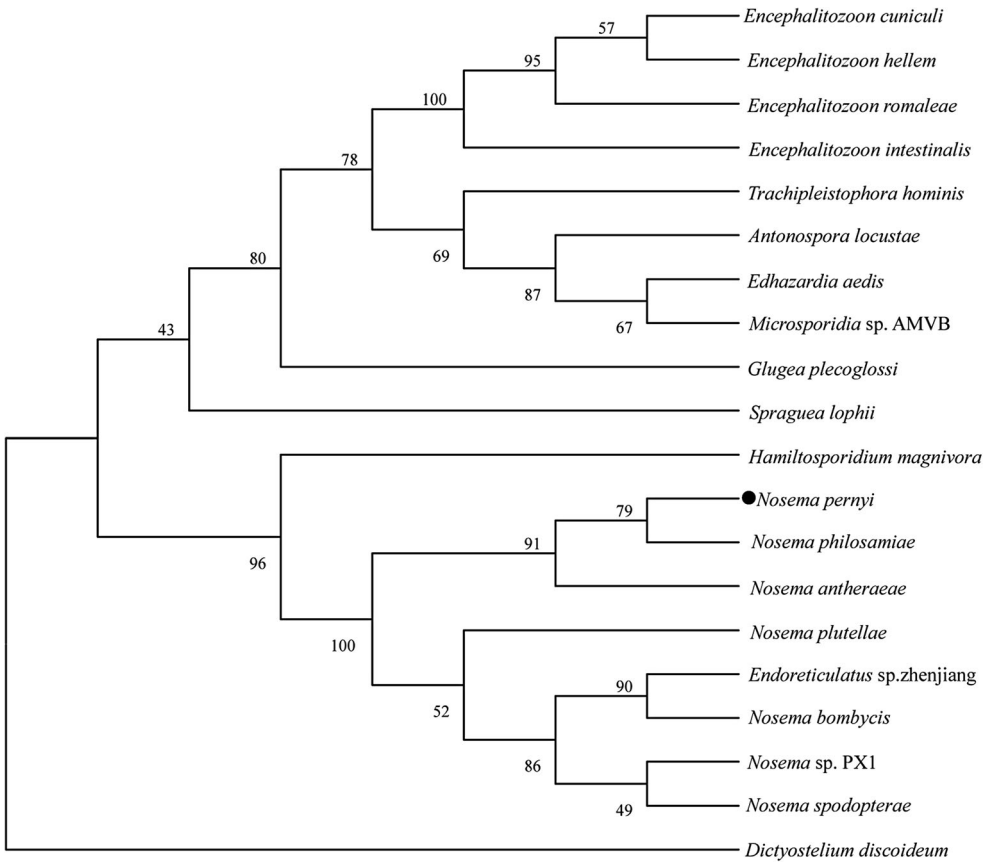

Fig. 3 Maximum likelihood phylogeny based on combined α- and β-*tubulin* gene sequences

fungal phylogenetic research. But each gene has its strengths and weaknesses; in order to get a credible result, comprehensive phylogeny will emerge from the analysis of a single gene. Tubulins are widely used as molecular markers for the original research of microsporidia and the evolutionary relationships among the major lineages of fungi (Keeling 2003; Zhu et al. 2013). There is a high level of structural and sequence conservation among actin proteins between eukaryotic and bacterial homologues. But the evolution of actin is characterized by independent expansions and contractions across the eukaryotic tree of life (Lahr et al. 2011).

In this study, ML tree based on α-*tubulin*, β-*tubulin* genes, *E. cuniculi*, *Encephalitozoon hellem*, *Encephalitozoon romaleae*, and *E. intestinalis*, which parasitize mammals, were grouped together, and were distantly related to *Nosema* species that parasitize only Lepidoptera. Both molecular and morphological evidence indicate that *A. locustae* is not a member of the *Nosema* genus based on small subunit rRNA (Slamovits

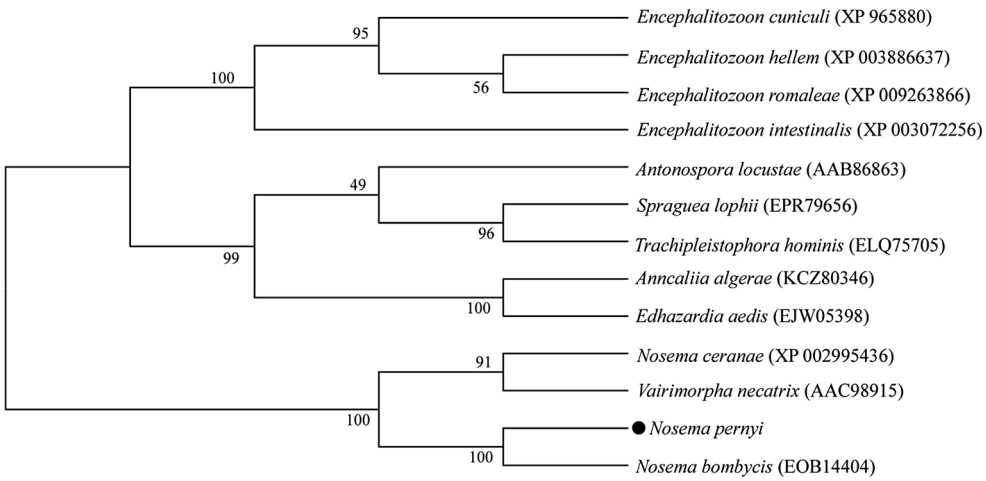

Fig. 4 Phylogenetic analysis of actin protein showing the relationship of *N. pernyi* with other 12 microsporidia. Phylogenetic tree was constructed by the neighbor-joining method

et al. 2004). The results based on the *tubulin* genes in our research are consistent with that of the previous study. Some studies have analyzed the relationship between *N. antheraeae* and other microsporidia using SSU rRNA, RPB1, and tubulin sequences. *N. antheraeae* has a close relationship with *N. bombycis*, both of them are the parasites of two economically important silk moths (Wang et al. 2006). In this study, *N. pernyi* belongs to the *Nosema* genus and has a closer relationship with *N. antheraeae* and *N. philosamiae*. The host of *N. philosamiae* is *P. cynthia ricini*, another wild silk worm that can be infected by *N. pernyi*. Microsporidian parasites of *A. pernyi* and *P. cynthia* can infect each other, but neither of these can infect *B. mori*, may be that is why there is a closer relationship between *N. philosamiae* and *N. pernyi* compared with *N. bombycis*. This result also is supported by phylogenetic analysis based on amino acid sequence of the *actin* gene. In conclusion, based on the evidence from morphological characteristics and phylogenetic analyses, *N. pernyi* is similar to *N. bombycis*, *N. philosamiae*, and *N. antheraeae*, and is correctly assigned to the *Nosema* group.

In summary, we have learned the symptoms of microsporidiosis in *A. pernyi*; different tissues of infected larval have been dissected in the fifth instar. Light and electron microscopes were used to observe the mature spores of *N. pernyi*. Transmission electron microscopy showed the spore wall, nucleus, and polar tube. From the constructed cDNA library, 864 clones were sequenced and 626 high-quality ESTs were assembled into 197 unigenes. One hundred and thirty-one ESTs have been sequenced to 3 end, and 90 genes showed significant homology to known genes in the NCBI database. Using *α-tubulin*, *β-tubulin*, and *actin* genes, we constructed two phylogenetic tree showing *N. pernyi* was closely related to *N. bombycis*, *N. philosamiae*, and other *Nosema* species. According to these morphological and molecular characteristics, we have a deeper understanding of *N. pernyi* which parasitize the Chinese oak silkworm. Further research is needed to ensure the genes function and pathophysiological mechanisms in host-parasite interactions.

Acknowledgments This project was supported by grants from the National Modern Agriculture Industry Technology System Construction Project (Silkworm and Mulberry) (No. CARS-22), Key task project in Science and Technology of Liaoning province, and the Scientific Research Project for Education Department of Liaoning province (No. 2014476), Cultivation Plan for Youth Agricultural Science and Technology Innovative Talents of Liaoning Province (No. 2014040).

References

Bhat SA, Bashir I, Kamili AS (2009) Microsporidiosis of silkworm, Bombyx mori L. (Lepidoptera-Bombycidae): a review. Afr J Agric Res 4:1519–1523

Bhat SA, Nataraju B (2005) A report on the impact of a microsporidian parasite on lamerin breed of the silkworm *Bombyx mori* L. Int J Ind Entomol 10:143–145

Cheney SA, Lafranchi-Tristem NJ, Bourges D, Canning EU (2001) Relationships of microsporidian genera, with emphasis on the polysporous genera, revealed by sequences of the largest subunit of RNA polymerase II (RPB1). J Eukaryot Microbiol 48(1):111–117

Cornman RS et al (2009) Genomic analyses of the microsporidian *Nosema ceranae*, an emergent pathogen of honey bees. PLoS Pathog 5(6):e1000466

Corradi N, Gangaeva A, Keeling PJ (2008) Comparative profiling of overlapping transcription in the compacted genomes of microsporidia *Antonospora locustae* and *Encephalitozoon cuniculi*. Genomics 91(4):388–393

Didier ES (2005) Microsporidiosis: an emerging and opportunistic infection in humans and animals. Acta Trop 94(1):61–76

Franzen C (2008) Microsporidia: a review of 150 years of research. Open Parasitol J 2:1–34

Jiang YR et al (2011) Development of a PCR-based method for detection of *Nosema pernyi*. Afr J Microbiol Res 5(24):4065–4070

Keeling PJ (2003) Congruent evidence from α-tubulin and β-tubulin gene phylogenies for a zygomycete origin of microsporidia. Fungal Genet Biol 38(3):298–309

Keeling PJ, Slamovits CH (2004) Simplicity and complexity of microsporidian genomes. Eukaryot Cell 3(6):1363–1369

Lahr DJ, Nguyen TB, Barbero E, Katz LA (2011) Evolution of the actin gene family in testate *lobose amoebae* (Arcellinida) is characterized by two distinct clades of paralogs and recent independent expansions. Mol Biol Evol 28(1):223–236

Li JN, Wang AR, Wang LM, Xu FG, Liu XG (2005) Infection and reproduction of *Nosema pernyi* in primary culture cell of Tussah ovary. J Shenyang Agric Univ 36(4):451–453

Liu HD, Ding ST, Qin QZ, Tang J, Liu L, Peng HM (2015) Morphological and phylogenetic analysis of *Nosema* sp. HR (Microsporidia, Nosematidae): a new microsporidian pathogen of *Histia rhodope* Cramer (Lepidoptera, Zygaenidae). Parasitol Res 114(3):983–988

Liu HD, Pan GQ, Li T, Huang W, Luo B, Zhou ZY (2012) Ultrastructure, chromosomal karyo type, and molecular phylogeny of a new isolate of microsporidian *Vairimorpha* sp. BM (Microsporidia, Nosematidae) from *Bombyx mori* in China. Parasitol Res 110(1): 205–210

Liu YQ, Li YP, Li XS, Qin L (2010) The origin and dispersal of the domesticated Chinese oak silkworm, *Antheraea pernyi*, in China: a reconstruction based on ancient texts. J Insect Sci 10(180):1–10

Mardis ER (2008) Next-generation DNA sequencing methods. Annu Rev Genomics Hum Genet 9:387–402

Nageswara-Rao S, Muthulakshmi M, Kanginakudru S, Nagaraju J (2004) Phylogenetic relationships of three new microsporidian isolates from the silkworm, *Bombyx mori*. J Invertebr Pathol 86(3):87–95

O'Mahony EM, Tay WT, Paxton RJ (2007) Multiple rRNA variants in a single spore of the microsporidian *Nosema bombi*. J Eukaryot Microbiol 54(1):103–109

Phukon M, Namdev R, Deka D, Modi MK, Sen P (2012) Construction of cDNA library and preliminary analysis of expressed sequence tags from tea plant [*Camellia sinensis* (L) O. Kuntze]. Gene 506(1):202–206

Schottelius J, Schmetz C, Kock NP, Schüler T, Sobottka I, Fleischer B (2000) Presentation by scanning electron microscopy of the life cycle of microsporidia of the genus *Encephalitozoon*. Microbes Infect 2(12):1401–1406

Slamovits CH, Williams BA, Keeling PJ (2004) Transfer of *Nosema locustae* (Microsporidia) to *Antonospora locustae* n. comb. Based on molecular and ultrastructural data. J Eukaryot Microbiol 51(2): 207–213

Sprague V, Becnel JJ, Hazard EI (1992) Taxonomy of phylum Microspora. Crit Rev Microbiol 18(5-6):285–395

Su GM, Ding J, Wen JZ (1992) Study on the pebrine pathogens in Chinese Tussah silkworm, *Antheraea pernyi* Guérin-Méneville. Acta Sericologica Sinica 2:1–34

Tamura K, Peterson D, Peterson N, Stecher G, Nei M, Kumar S (2011) MEGA5: molecular evolutionary genetics analysis using maximum likelihood, evolutionary distance, and maximum parsimony methods. Mol Biol Evol 28(10):2731–2739

Tanabe Y, O'Donnell K, Saikawa M, Sugiyama J (2000) Molecular phylogeny of parasitic Zygomycota (Dimargaritales, Zoopagales) based on nuclear small subunit ribosomal DNA sequences. Mol Phylogenet Evol 16(2):253–262

Tokarev YS, Voronin VN, Seliverstova EV, Pavlova OA, Issi IV (2010) Life cycle, ultrastructure, and molecular phylogeny of Crispospora chironomi g.n. sp.n. (Microsporidia: Terresporidia), a parasite of Chironomus plumosus L. (Diptera: Chironomidae). Parasitol Res 107(6):1381–1389

Velide L, Bhagavanulu M (2012) Estimation of efficient concenteration of Bavistin in controlling microsporidiasis and improving cocoon characters in *Anthereae mylitta* drury (Andhra local ecorace). Int J Plant Anim Environ Sci 2(1):177–182

Velide L, Rao AP (2011) Studies on the impact of microsporidiosis on tropical tasar silkworm *Anthereae mylitta* Drury. J Appl Biosci 44: 2994–2999

Wang LL, Chen KP, Zhang Z, Yao Q, Gao GT, Zhao Y (2006) Phylogenetic analysis of *Nosema antheraeae* (Microsporidia) isolated from Chinese oak silkworm, *Antheraea pernyi*. J Eukaryot Microbiol 53(4):310–313

Williams BA, Hirt RP, Lucocq JM, Embley TM (2002) A mitochondrial remnant in the microsporidian *Trachipleistophora hominis*. Nature 418(6900):865–869

Wittner M, Weiss LM (1999) Microsporidia and microsporidiosis. American Society for Microbiology

Wu ZL et al (2008) Proteomic analysis of spore wall proteins and identification of two spore wall proteins from *Nosema bombycis* (Microsporidia). Proteomics 8(12):2447–2461

Xu JS, Wang M, Zhang XY, Tang FH, Pan GQ, Zhou ZY (2010) Identification of *NbME* MITE families: potential molecular markers in the microsporidia *Nosema bombycis*. J Invertebr Pathol 103(1): 48–52

Yang L et al (2009) Construction and analysis of bacterial artificial chromosome (BAC) library of *Nosema bombycis*. Sci Sericulture 2:314–219

Zhou RQ, Xia QY, Huang HC, Lai M, Wang ZX (2011) Construction of a cDNA library from female adult of *Toxocara canis*, and analysis of EST and immune-related genes expressions. Exp Parasitol 129(2): 120–126

Zhu F et al (2011) A new isolate of Nosema sp. (Microsporidia, Nosematidae) from Phyllobrotica armata Baly (Coleoptera, Chrysomelidae) from China. J Invertebr Pathol 106(2):339–342

Zhu F, Shen ZY, Xu L, Guo XJ (2013) Molecular characteristics of the alpha-and beta-tubulin genes of Nosema philosamiae. Folia Parasitol 60(5):411–415